J. Shanghai Jiao Tong Univ. (Sci.), 2021, 26(6): 765-773
https://doi.org/10.1007/s12204-020-2237-5

Experimental Study on Medium and Low Cycle Fatigue Properties of Cast Steel GS20Mn5V

*JIN Hui** (靳　慧), *MO Jianhua* (莫建华), *SUN Sijia* (孙思嘉), *ZHAO Jing* (赵　静)
(Jiangsu Key Laboratory of Engineering Mechanics & Key Laboratory of Concrete and Prestressed Concrete Structures of Ministry of Education, School of Civil Engineering, Southeast University, Nanjing 210096, China)

Abstract: Owing to the remarkable advantages in mechanical behavior, cast steel nodes have been widely used in static structures. Nowadays, cast steel nodes also gain increasing popularity due to the superior fatigue performance in dynamic structures, but they are not yet widely used because the fatigue properties of cast steel are not well understood. In this paper, the fatigue test of cast steel GS20Mn5V commonly used in steel castings is carried out. The strength of medium and low cycle fatigue and the fatigue limit are obtained. The feasibility of the estimated *S-N* (fatigue stress versus life) curve is tested. The double logarithmic linear model (DLLM) and the reversed generalized Pareto model (RGPM) are used to fit the experimental data, and the comparison is made. The *P-S-N* (the relationship between fatigue stress and life at different survival rates) curve obtained by the RGPM is proposed. The results show that the estimated *S-N* curve is not suitable for low cycle fatigue life, fitting the experimental data with the RGPM is the best, and obtaining the *P-S-N* curve from the RGPM is feasible.
Key words: cast steel GS20Mn5V, fatigue test, double logarithmic linear model (DLLM), reversed generalize Pareto model (RGPM), *S-N* curve, *P-S-N* curve
CLC number: TG 142, TU 391　　**Document code:** A

0 Introduction

Cast steel nodes have various types and stable mechanical behavior. In recent years, cast steel nodes have been used widely in the junctions with large internal forces and complex geometry for the large structures under static load, such as stadiums, airport terminals, and exhibition centers. Actually, owing to the superior fatigue performance of cast steel, many structures under fatigue load are inclined to cast steel nodes, from ocean engineering structures to bridges and high-rise buildings, where the fatigue failure is the main detriment.

The fatigue behavior of cast steel joints and their weld properties are not adequately studied yet. Nevertheless, the main relevant researches have been done. Haldimann-Sturn and Nussaumer[1] studied the fatigue properties of the cast steel joints and the traditional welded joints, and investigated the allowable initial defect sizes. Jin et al.[2-3] conducted the numerical calculations to study the fatigue of cast steel nodes in a tower steel structure. Guo et al.[4-7] studied the fatigue performance and fatigue failure mechanism of cast steel joints through a series of experiments. Jin[8] and Sun et al.[9] optimized the original fatigue strength analysis method, and applied different fatigue strength analysis methods to the fatigue analysis of cast steel joints. Gong[10] and Li et al.[11-12] studied the effect of casting defects on the fatigue properties of cast steel joints. Zhu et al.[13-15] studied the effects of temperature, microstructure and other factors on the fatigue properties of the cast steel joints.

The fatigue data of cast steels are still limited, which cannot meet the fatigue design requirement of cast steel joints. In civil engineering practices, cast steel GS20Mn5V is a common casting material for cast steel joints. In this study, the fatigue test is carried out in order to research the fatigue performances of cast steel GS20Mn5V. In the experiment, 44 samples are cut from three casting nodes (I, II, III). Only the data of Nodes II and III are concluded in the fatigue test, in which the group method is used to investigate the fatigue strength of medium and low cycle fatigue and the

Received: 2019-05-20　**Accepted:** 2019-09-03
Foundation item: the National Key Research and Development Program of China (No. 2017YFC0805100), the National Natural Science Foundation of China (No. 51578137), the Priority Academic Program Development of the Jiangsu Higher Education Institutions, and the Open Research Fund Program of Jiangsu Key Laboratory of Engineering Mechanics
***E-mail:** jinhui@seu.edu.cn

small subsample fluctuation method is used to investigate the fatigue limit. Firstly, the double logarithmic linear model (DLLM) is used to fit the test data, and the fitting results are compared with the S-N curves constructed by other simplified methods. Then, the reversed generalized Pareto model (RGPM) is proposed to fit the test data, and the parameters in the RGPM are obtained by two ways: order statistic, and regression method. The absolute fitting errors of the DLLM and RGPM are compared. Lastly, the P-S-N curves are obtained by the RGPM based on order statistic.

1 Experimental Procedure

1.1 Selection and Fabrication of the Test Specimens

In China, casting components are divided by five grades based on the amount and size of defects according to nondestructive testing standard[16]: Grade 1 is the best, and Grade 5 is the worst. In civil engineering practices, Grades 1, 2 and 3 are commonly used.

Figure 1 shows the fabrication of the test specimens. When the nodes are cast (Fig. 1(a)), the same pouring material is used to cast thick plates separately (Fig. 1(b)). The thick plate is cut into small cylinder specimens (Fig. 1(c)) which are then processed into the test specimen like (Fig. 1(d)). Totally, there are three groups of specimens. The defects inside the test piece are examined by industrial X-ray, and no obvious macro defects are found. The size of final test specimen is shown in Fig. 2.

(a) Cast steel nodes (b) Casting thick plates

(c) Cutting (d) Specimens

Fig. 1 Cast steel nodes and preparation of specimens

1.2 Test Instrumentation and Loading

PLG-100 high-frequency fatigue testing machine is shown in Fig. 3. The specimens are placed symmetrically in the fixture, and the bolts are tightened to prevent the specimens from moving. The specimens are under axial tension-compression with constant amplitude at different stress levels. The test is stopped when the area of the fatigue crack exceeds 50% of the specimen section.

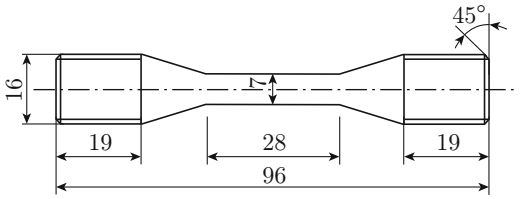

Fig. 2 Specimen size (mm)

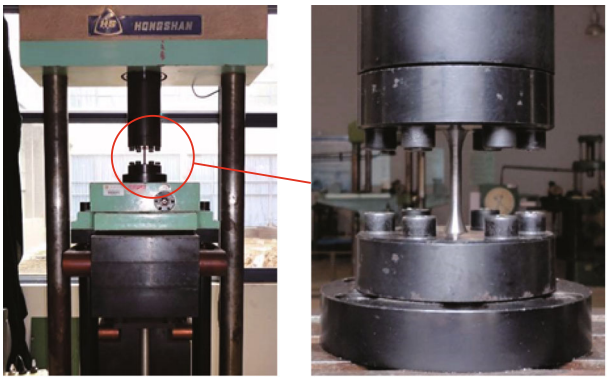

Fig. 3 High-frequency fatigue testing machine and its clamping method

1.3 Group Method to Test the Medium and Low Cycle Fatigue Life Ranges

The group method is used to test the fatigue life ranges of the medium and low cycles. The fatigue life range corresponds to the oblique line section of the S-N curve. The minimum sample number $n_{\min}$ in each group is determined by the life variation coefficient v at the test level[17-18]:

$$v = \frac{\sigma_x}{\bar{x}}, \tag{1}$$

where σ_x is the standard deviation of fatigue life, and $\bar{x}$ is the average logarithm value of fatigue life. When the confidence level γ is fixed, the bigger the life variation coefficient is, the larger the minimum sample number is (Fig. 4)[17].

The number of stress levels is determined by[17-18]

$$r = \frac{L_{SN}}{\sqrt{L_{SS}L_{NN}}}, \tag{2}$$

where

$$L_{SS} = \sum_{j=1}^{l}(\lg S_j)^2 - \frac{1}{l}\Big(\sum_{j=1}^{l}\lg S_j\Big)^2,$$

$$L_{NN} = \sum_{j=1}^{l}(\lg N_j)^2 - \frac{1}{l}\Big(\sum_{j=1}^{l}\lg N_j\Big)^2,$$

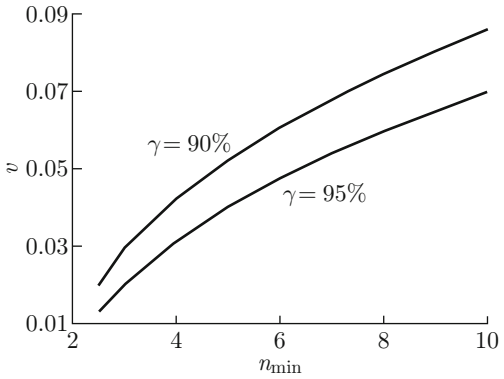

Fig. 4 Line graphs of determining the minimum sample number

$$L_{SN} = \sum_{j=1}^{l} \lg S_j \lg N_j - \frac{1}{l}\Big(\sum_{j=1}^{l} \lg S_j\Big)\Big(\sum_{j=1}^{l} \lg N_j\Big),$$

$$\lg N = a + b \lg S,$$

$$a = \frac{1}{l}\sum_{j=1}^{l} \lg N_j - \frac{b}{l}\sum_{j=1}^{l} \lg S_j,$$

$$b = \frac{\sum\limits_{j=1}^{l} \lg S_j \lg N_j - \frac{1}{l}\Big(\sum\limits_{j=1}^{l} \lg S_j\Big)\Big(\sum\limits_{j=1}^{l} \lg N_j\Big)}{\sum\limits_{j=1}^{l} (\lg S_j)^2 - \frac{1}{l}\Big(\sum\limits_{j=1}^{l} \lg S_j\Big)^2},$$

r is the linear correlation of the stress and life, S_j denotes the stress value at the jth stress level, $\lg N_j$ denotes the logarithm average life at S_j, and l denotes the total number of stress levels. As the absolute value of r comes to l, the relationship between $\lg S$ and $\lg N$ becomes linear. The linear fitting of $\lg S$ and $\lg N$ needs enough linear correlation with r. When the number of stress levels is 3, the minimum value of r for linear fit should be bigger than 0.997. When the number of stress levels is 4, the minimum value of r should be bigger than 0.95[17].

1.4 Up-and-Down Method to Test the Fatigue Limit

In consideration of the test specimen number and the test time, the up-and-down method is used to measure the fatigue limit of cast steel GS20Mn5V. The test is started at the roughly estimated fatigue limit S_{-1}, and the fatigue life limit is set to 2×10^6. If the first test specimen fails before 2×10^6 cycles, the next specimen will be tested with a decrease of 4%—6% for the stress level. If the first test specimen does not fail above 2×10^6 cycles, the next specimen will be tested with an increase of 4%—6% for the stress level. The same process is taken for the rest specimens. Figure 5 shows the up-and-down method.

The data before the first adverse results (one point is ×, and the adjacent one is ○) should be discarded,

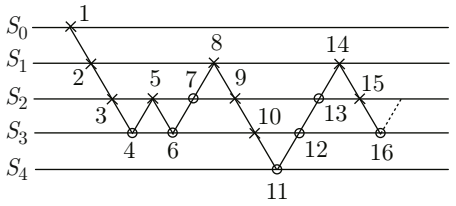

Fig. 5 Up-and-down method

such as Points 1 and 2 in Fig. 5; the corresponding test specimens are invalid. Points 3 and 4 are two adverse points, and they can be matched into one couple. The average value $(S_3 + S_4)/2$ is regarded as one of the estimated fatigue limits. The 8th specimen (Point 8 in Fig. 5) is the same as Point 2 (invalid), and because the test value of Point 2 is not used, the data point 2 can replace the 8th point. The same process can be applied to the other invalid specimens, but each data point can only be used once. Using the matched couples of all effective points, the average value of the fatigue limit is calculated as

$$S_{-1} = \frac{1}{k}\sum_{i=1}^{k} S_{-1i}, \tag{3}$$

where k is the number of the matched couples, and S_{-1i} is the fatigue limit of the ith couple. Here, $S_{-11} = (S_3 + S_4)/2$, $S_{-12} = (S_5 + S_6)/2$. The standard deviation of the fatigue limit is calculated as

$$\sigma_{S_{-1}} = \left[\frac{1}{k-1}\sum_{i=1}^{k} S_{-1i}^2 - \frac{1}{k(k-1)}\Big(\sum_{i=1}^{k} S_{-1i}\Big)^2\right]^{\frac{1}{2}}. \tag{4}$$

2 Fitting Results of the DLLM

2.1 Medium and Low Cycle Fatigue Life Values

The specimens of three groups can be treated as an integral sample. All the test data distribute in a certain range, as shown in Fig. 6. An average curve is fitted

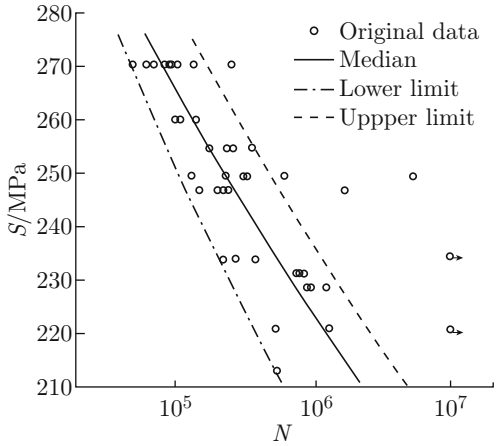

Fig. 6 Distribution range of casting fatigue life values

with all the valid data, and the boundary curves are fitted with the boundary data.

The average value equation (S in unit MPa) of S-N curve for the integral sample is

$$\lg N = 36.693\,3 - 13.070\,4 \lg S. \tag{5}$$

If the logarithmic fatigue life $\lg N$ obtained by Eq. (5) is considered as the average value at a certain amplitude stress level, the life distribution is analyzed. The difference of the logarithmic fatigue life values is denoted as $\bar{X} = \lg N - \lg \bar{N}$ (valid test data). According to the test data calculation, the average value of $\bar{X}$ is 0.000 26, and the standard deviation of $\bar{X}$ is 0.192 6. An increment $\Delta\bar{X}$ is set as 0.1. Here, the number of test specimens is denoted as n. The distribution of n corresponding with $\lg N - \lg \bar{N}$ is shown in Fig. 7, which matches the normal distribution curve with an average value of 0.000 26 and a standard deviation of 0.192 6. The life distribution can be considered as a logarithm normal distribution.

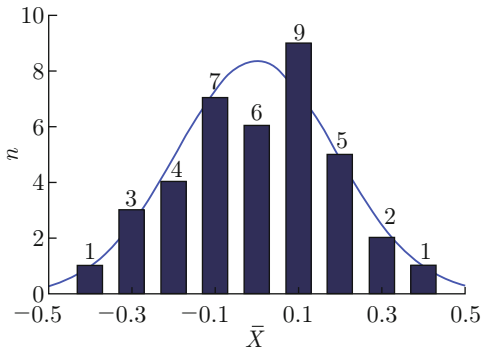

Fig. 7 Distribution of fatigue life values

The amplitude stress levels are divided into three ranges (270.4 MPa, 270.4 MPa), (245 MPa, 260 MPa) and (210 MPa, 235 MPa), with 6, 16 and 12 test datasets respectively; the corresponding standard deviations of the logarithmic fatigue life difference $\bar{X}$ are 0.141 4, 0.182 7 and 0.245 2, respectively.

2.2 Fatigue Limit

At the beginning of the experiment, owing to the failure of accurately estimating the required number of the samples of Node I, the material fatigue test data of Node I are not complete. Therefore, only the test data of Nodes II and III are listed, as shown in Figs. 8 and 9, respectively.

As seen from Fig. 8, the first adverse results occur on Specimens 3 and 4, so Specimens 1 and 2 are invalid and should be neglected. However, the amplitude stress value of the one following Specimen 7 is the same as that of Specimen 2, so the unused data of Specimen 2 can be used as the 8th data point. In the same way, the data of Specimen 1 can be used as the 11th data point. According to Eqs. (3) and (4), the average value

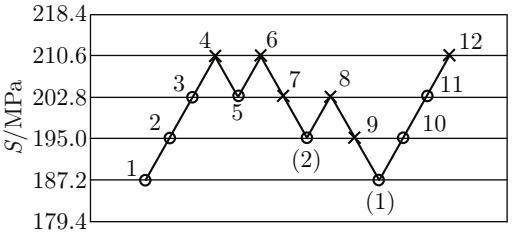

Fig. 8 Fatigue limit of Node II

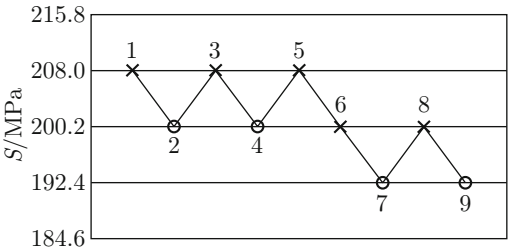

Fig. 9 Fatigue limit of Node III

of fatigue limit S_{-1} is 202.1 MPa, and the standard deviation $\sigma_{S_{-1}}$ is 7.012 MPa.

As seen from Fig. 9, Specimen 5 has no matched points, so the test data of Specimen 5 are neglected. According to the four matched couple data points, the average value of the fatigue limit S_{-1} is 200.2 MPa and the standard deviation $\sigma_{S_{-1}}$ is 4.503 MPa. The average values of the fatigue limits of Nodes II and III are 201 MPa.

2.3 Integral S-N Curve

The integral S-N curve of cast steel GS20Mn5V is drawn with the maximum fatigue limit test value 208.0 MPa as the upper limit and the minimum fatigue limit test value 191.1 MPa as the lower limit, as shown in Fig. 10.

Before this fatigue test study of cast steel GS20Mn5V, the engineers approximately estimate its

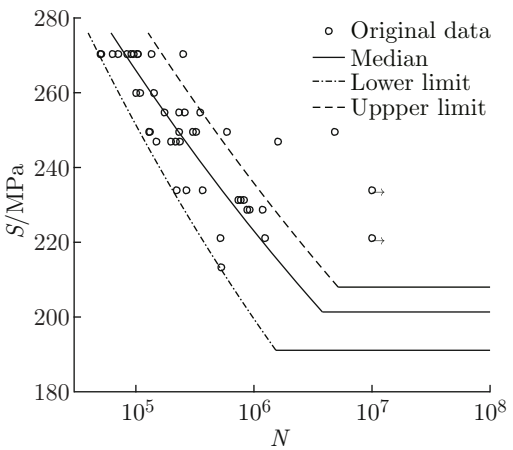

Fig. 10 Distribution range of the integral S-N curve

fatigue strength with the yield limit when there is not available fatigue data. Reference [19] presented the details of approximate evaluation method, in which the estimated result is $\lg N = 25.9535 - 8.5183 \lg S$ (S in unit MPa) with a fatigue limit of 220 MPa.

In this study, all the integral S-N curves are plotted in Fig. 11 to discuss the precision of approximate evaluation method, in which the cross point between theoretical curve and upper limit curve is (18 462, 268 MPa), and the cross point between theoretical curve and median curve is (717 960, 228 MPa). As seen from Fig. 11, when the stress amplitude is bigger than 268 MPa, it is very risky to apply the estimated S-N curve to lower-cycle fatigue, because it exceeds the upper limit of the test data. When the stress amplitude is lower than 268 MPa, the estimated S-N curve is more conservative than the upper limit, but it is a little complicated than the median S-N curve and should be treated with caution. The estimated fatigue limit 220 MPa is 5.7% bigger than the maximum test value 208.0 MPa. As a result, the estimated S-N should be treated carefully in engineering application.

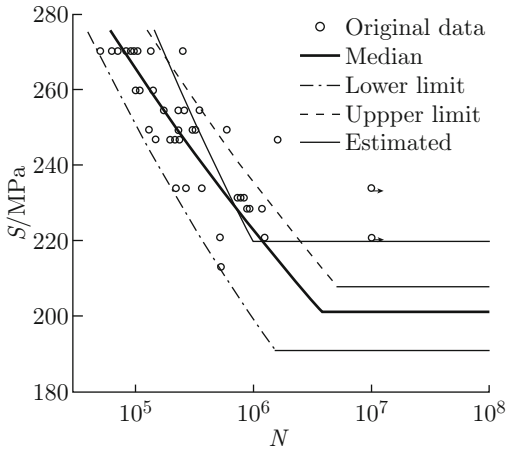

Fig. 11 Comparison of the integral S-N curves

The integral S-N curve based on test data and the comparison result with the estimated S-N curve can offer an important reference for the fatigue strength assessment of similar material in engineering application.

Now the S-N curve has been obtained, while the P-S-N curve has not been obtained because of lack of available data.

3 Fitting Results of the RGPM

RGPM is based on physical and statistical considerations[20]. These considerations require that fatigue models should satisfy the following conditions. ① Models should take into account the fact that fatigue life is governed by the weakest link principle, and the weakness of a sub-piece is determined by the size of its largest crack and the stress it is subjected to. ② Models must be stable with respect to minimum operations. ③ Models must take into account the positive characters of fatigue life and stress level. ④ The distributions of fatigue life given stress level should be compatible with the distribution of the stress level given life. If $F_X(x, y)$ is the cumulative distribution function of X given y, and $F_Y(y, x)$ is the cumulative distribution function of Y given x, then $F_X(x, y) = F_Y(y, x)$. A reasonable model (here, H represents the failure percent, x is taken as the fatigue life, and y is taken as the stress level) based on the reversed generalized Pareto distribution is

$$H(x, y) = [\beta + \sigma'(x - \delta)(y - \rho)]^{1/\alpha}, \tag{6}$$

where ρ is the endurance limit (i.e., fatigue failure does not occur below ρ), δ is a minimum life that can be guaranteed for all the specimens, σ' is a combined scale factor for fatigue life and stress level, β is associated with the zero percentile (if β is zero, the zero-percentile curve degenerates to two straight lines parallel to the x and the y axes), and $1/\alpha$ is the shape parameter.

Let A, B, C and D be the parameters derived from $\sigma' = A$, $\delta = -C/A$, $\rho = -B/A$, $\beta = D - BC/A$. Define P as the survival rate, and the fatigue failure as $p = 1 - P$. When the failure rate is $p = H$, the S-N curve equation is obtained as

$$X_p = \frac{p^\alpha - D - Cy}{Ay + B}. \tag{7}$$

From Eq. (7), it is can be seen that the smaller the absolute value of A is, the more linear the curve is. When $A = 0$, the S-N curve equation becomes linear. It is similar to the convention method.

Suppose that there are L stress levels $y_1 < y_2 < \cdots < y_L$, and for each stress level y_j, there are n_j values of X, which are denote by $x_{1j}, x_{2j}, \cdots, x_{n_j j}$. Thus, x_{ij} is the ith observed life for the stress level y_j. Without loss of generality, assume that $x_{1j} < x_{2j} < \cdots < x_{n_j j}$; x_{ij} is the ith order statistic of the life associated with the jth stress level y_j. From Eq. (7), x_{ij} can be approximated:

$$x_{ij} = \frac{p_{ij}^\alpha - D - Cy_i}{Ay_j + B}, \tag{8}$$

with $p_{ij} = (i - 0.5)/n_j$.

Elemental percentile method is used to estimate the parameters[20]. The elemental percentile method is a two-stage procedure. In the first stage, α is estimated. The estimate of α does not computationally depend on the values of the other parameters. In the second stage, the other four parameters are estimated.

3.1 Estimation of α

According to the existing data, the statistics are considered as

$$Z_j(i, r, s, t) = \frac{x_{ij} - x_{rj}}{x_{sj} - x_{tj}}, \tag{9}$$

with

$$j \in \mathbf{Z}; i, r, s, t \in \{1, 2, \cdots, n_j\}; x_{sj} \neq x_{tj}.$$

Substituting Eq. (8) into Eq. (9) can yield

$$Z_j(i, r, s, t) = \frac{p_{ij}^{\alpha} - p_{rj}^{\alpha}}{p_{sj}^{\alpha} - p_{ij}^{\alpha}}. \tag{10}$$

The value of α can be estimated by Eq. (10). Note that Eq. (10) is for any stress level and any points i, r, s, t associated with and satisfying Eq. (9). Owing to setting $r = s$, Eq. (9) can still be satisfied, so the value of α can be estimated by only three distinct points. It is different from the linear method which requires at least 6 data points for each stress level. Castillo and Hadi[20] have proved that the fitting result is better when

$$i = 1, \quad r = [(n_j + 1)/2], \quad t = n,$$

and there is one α for one stress level. Let $\widehat{\alpha}_j$ be an estimate of α_j at the jth stress level, and $\widehat{\alpha}$ be an estimate of α. We take the weighted mean as

$$\widehat{\alpha} = \sum_{j=1}^{L} n_j \widehat{\alpha}_j \Big/ \sum_{j=1}^{L} n_j. \tag{11}$$

All of the available test data are shown in Fig. 12. From Eq. (11), the estimate of α can be got:

$$\widehat{\alpha} = \frac{62.991\,4}{35} \approx 1.8.$$

3.2 Estimation of the Parameters

3.2.1 *Estimation by Order Statistics*

As shown in Fig. 12, there are 8 stress levels in the experiment (the number of valid test data points for each stress level is 10, 3, 4, 6, 3, 3, 3, 3). Firstly, two stress levels y_j and y_k, and two test data for each stress level x_{ij}, x_{rj}, x_{ik} or x_{rk} are chosen. From Eq. (8), an equation group is obtained as

$$x_{ij} = \frac{p_{ij}^{\alpha} - D - Cy_j}{Ay_j + B}, \quad x_{rj} = \frac{p_{rj}^{\alpha} - D - Cy_j}{Ay_j + B}, \tag{12}$$

$$x_{ik} = \frac{p_{ik}^{\alpha} - D - Cy_k}{Ay_k + B}, \quad x_{rk} = \frac{p_{rk}^{\alpha} - D - Cy_k}{Ay_k + B}. \tag{13}$$

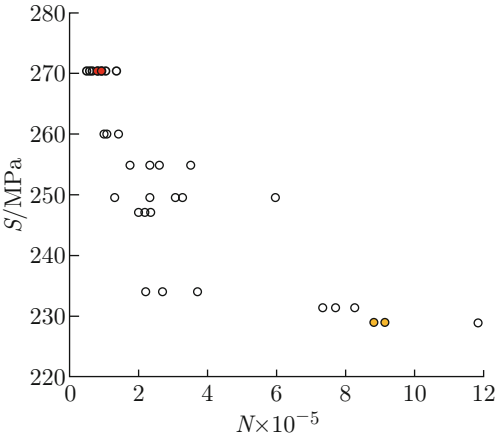

Fig. 12 Valid fatigue test data

The parameters A, B, C and D are obtained by solving Eqs. (12) and (13). It has been proved that the best estimators are obtained from the furthest apart stress levels[20], so $j = 1$ and $k = 8$ are set in the existing data.

In order to reduce the workload without loss of generality, several representative test data points in the 1st and 8th stress levels are chosen (the numbers in the following parentheses successively represent the values of j and i). ① Two median life of the 1st and 8th stress levels: (1, 5), (1, 6), (8, 1), (8, 2) (see the red and yellow points in Fig. 12); ② The maximum and minimum life of the 1st and 8th stress levels: (1, 1), (1, 10), (8, 1), (8, 3); ③ Two minimum life of the 1st and 8th stress levels: (1, 1), (1, 2), (8, 1), (8, 2); ④ Two maximum life of the 1st and 8th stress levels: (1, 9), (1, 10), (8, 2), (8, 3).

Set survival rate $P = 0.5$ (failure rate $p = 0.5$). In order to obtain the estimated values of each parameter (for the S-N curves y_1, y_2, y_3 and y_4 corresponding to ①, ②, ③ and ④, see Table 1), the values of the above data points are substituted into Eqs. (12) and (13).

For comparing with the mean S-N curve, the form of Eq. (8) is changed into

$$y = \frac{0.5^{1.8} - D - Cx}{Ax + B}. \tag{14}$$

The curves y_1, y_2, y_3 and y_4 are shown in Fig. 13, where y is taken as the curve of DLLM. Obviously, y_1 and

Table 1 Estimated values of the parameters with four S-N curves

Method	A	B	C	D	σ'	δ	ρ	β
y_1	15.69×10^{-8}	-27.66×10^{-6}	14.97×10^{-2}	$-4\,150.50 \times 10^{-2}$	15.69×10^{-8}	$-954\,110.90$	176.29	-15.11
y_2	20.21×10^{-8}	-43.97×10^{-6}	34.69×10^{-3}	-991.13×10^{-2}	20.21×10^{-8}	$-171\,647.70$	217.56	-2.36
y_3	13.79×10^{-8}	-89.10×10^{-7}	44.63×10^{-2}	$-12\,210.17 \times 10^{-2}$	13.79×10^{-8}	$-3\,236\,403.19$	64.61	-93.26
y_4	89.11×10^{-9}	-18.78×10^{-6}	33.16×10^{-3}	-877.25×10^{-2}	89.11×10^{-9}	$-372\,124.34$	210.75	-1.78

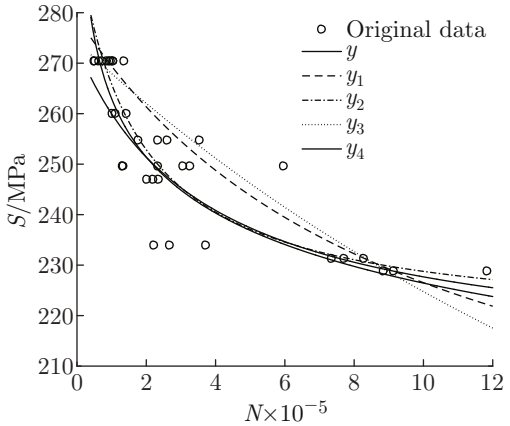

Fig. 13 Mean value S-N curves under different selecting methods

y_3 are further away from experimental data. In Table 1, the fatigue limit values of y_2 and y_4 are close to the experimental value 201.3 MPa, but the fatigue limit values of y_1 and y_3 are too far away from experimental value.

For quantity analysis, the sum of the absolute prediction errors is computed as

$$E=\sum_{j=1}^{L}\sum_{i=1}^{n_j}|x_{ij}-\widehat{x}_{ij}|, \tag{15}$$

where x_{ij} is taken as the test data value, and $\widehat{x}_{ij}$ is taken as the life estimated value by the curve equations. The absolute errors of the curve equations are listed in Table 2.

Table 2 Absolute errors of the fitting curves

Curve	$E\times10^{-6}$
y	3.1
y_1	4.3
y_2	3.0
y_3	4.9
y_4	3.4

The absolute errors of y_1 and y_3 are 37% bigger than the absolute error of DLLM. Here note that during estimating the parameters, the life values of the two data points selected in the 1st stress level of y_1 are close to each other: (84 700, 91 700). The life values of the two data points selected respectively in y_2 and y_4 are also close to each other: (49 900, 50 900) and (103 700, 134 800), but the difference between the two life values in y_4 is larger than the former.

According to the above results and the characters of the selected data points, it is can be inferred that for the same stress level, the larger the difference of life values of the selected data points is, the better the fitting results are. Considering the uncertainty of life data, more groups of data points are used to calculate the estimators, as shown in Table 3.

Table 3 Estimation of the parameters from different data points

Data points chosen		A	B	C	D
1st stress level	8th stress level				
(1, 1), (1, 10)	(8, 1), (8, 3)	2.02×10^{-7}	-4.40×10^{-5}	34.69×10^{-3}	-991.13×10^{-2}
(1, 2), (1, 9)	(8, 1), (8, 3)	2.86×10^{-7}	-6.39×10^{-5}	127.35×10^{-4}	-409.85×10^{-2}
(1, 3), (1, 8)	(8, 1), (8, 3)	2.67×10^{-7}	-5.96×10^{-5}	111.42×10^{-4}	-37.34×10^{-1}
(1, 4), (1, 7)	(8, 1), (8, 3)	2.66×10^{-7}	-5.93×10^{-5}	104.69×10^{-4}	-3.58×10^{0}
(1, 1), (1, 9)	(8, 1), (8, 3)	2.93×10^{-7}	-6.54×10^{-5}	12.05×10^{-3}	-394.17×10^{-2}
(1, 1), (1, 8)	(8, 1), (8, 3)	2.27×10^{-7}	-5.03×10^{-5}	15.33×10^{-3}	-469.31×10^{-2}
(1, 1), (1, 10)	(8, 1), (8, 3)	2.18×10^{-7}	-4.83×10^{-5}	15.76×10^{-3}	-478.95×10^{-2}
(1, 2), (1, 9)	(8, 1), (8, 3)	2.70×10^{-7}	-5.95×10^{-5}	316.65×10^{-4}	-92.17×10^{-1}
(1, 4), (1, 7)	(8, 1), (8, 3)	2.50×10^{-7}	-5.49×10^{-5}	293.98×10^{-4}	-869.85×10^{-2}
Mean value		2.53×10^{-7}	-5.61×10^{-5}	1.92×10^{-2}	-585.15×10^{-2}
Standard deviation		3.13×10^{-8}	7.27×10^{-6}	0.97×10^{-2}	261.60×10^{-2}
Variation coefficient		12.36×10^{-2}	-12.95×10^{-2}	50.64×10^{-2}	-44.71×10^{-2}

From the estimation by order statistics, the S-N curve equation with a failure rate of 0.5 by the mean values of A, B, C and D is

$$y_{\mathrm{O}}=\frac{p^{1.8}+5.85+5.61\times10^{-5}x}{2.53\times10^{-7}x+0.019\,2}. \tag{16}$$

For getting the best fitting results, regression estimates should be also used.

3.2.2 *Estimation by Regression Estimates*

For each data point, there is

$$y_jA+x_{ij}B+y_jC+D=p_{ij}^{\alpha},\quad j=1,2,\cdots,n_j. \tag{17}$$

It is can be seen from the above equation that the parameters A, B, C and D are all linear. Then, the method of least square linear regression can be used to estimate the values of A, B, C and D. The difference between this method and order statistics is that all the data points are applied, so the deviation is smaller in theory. The results of regression estimates are

$$A = 59.56 \times 10^{-9}, \quad B = -13.04 \times 10^{-6},$$
$$C = 60.81 \times 10^{-4}, \quad D = -158.39 \times 10^{-2}.$$

From the estimation by regression estimates, the curve equation is

$$y_{\mathrm{R}} = \frac{p^{1.8} + 1.589\,3 + 1.30 \times 10^{-5} x}{5.96 \times 10^{-8} x + 6.08 \times 10^{-3}}. \tag{18}$$

For getting better fitting results, the absolute errors of the above fitting equations will be compared in next section.

4 P-S-N Curve

Now, the above fitting curves and the original valid data are drawn, as shown in Fig. 14. The curves y, y_{O} and y_{R} represent Eqs. (14), (16) and (18), respectively. As seen from Fig. 14, compared with general linear fitting curves, the curves y_{O} and y_{R} are safer in the fatigue life located between 2×10^5 and 8×10^5. Then the absolute errors of y, y_{O} and y_{R} are listed in Table 4, showing that the curve y_{O} fits best.

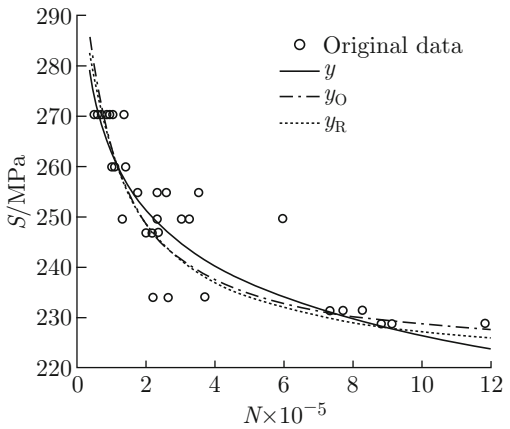

Fig. 14 Comparison of the estimation curves

Table 4 Absolute errors of the estimation curves

Curve	$E \times 10^{-6}$
y	3.12
y_{O}	2.89
y_{R}	3.16

The RGPM based on order statistic is proposed to obtain the P-S-N curves through changing the value of P. The curves are shown in Fig. 15.

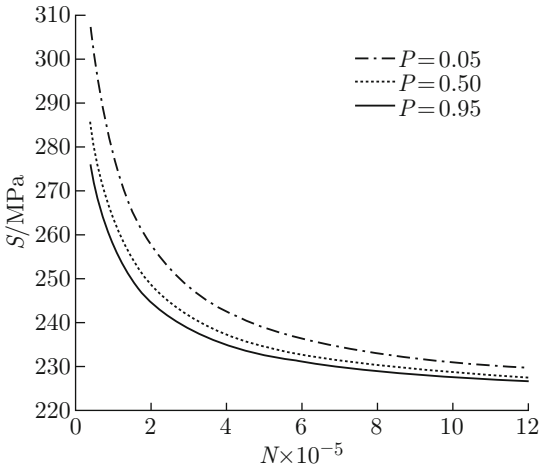

Fig. 15 Comparison of the P-S-N curves

The fatigue data of the stress level 270.4 MPa (the largest sample size 10 in this study) are used for validation of the P-S-N curves. For different survival rates, the relative error (denoted as e) between the experimental value and the calculated value according to Eq. (16) is shown in Fig. 16. The biggest relative error is less than 15%, so this method is recommended in absence of test data to obtain P-S-N for fatigue reliability analysis.

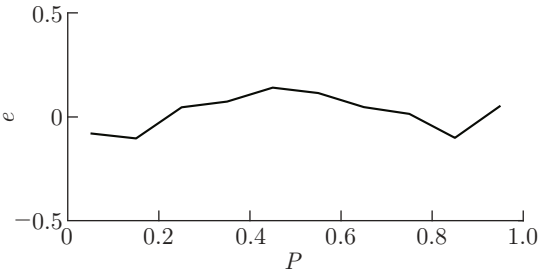

Fig. 16 Relative error of the P-S-N equation

5 Conclusion

The fatigue properties of cast steel GS20Mn5V are studied by fatigue test, and the following conclusions are got: the application of the estimated S-N curve in low-cycle fatigue is very dangerous and should be handled with caution in practical engineering; compared with the DLLM, the RGPM based on the order statistical method is more suitable for fitting test data; in the absence of test data, it is recommended to use the RGPM to obtain the P-S-N curve for fatigue reliability analysis.

The above characteristics of cast steel GS20Mn5V provide an important reference for its structural application under cyclic loading.

References

[1] HALDIMANN-STURN S C, NUSSAUMER A. Fatigue design of cast steel nodes in tubular bridge structures [J]. *International Journal of Fatigue*, 2008, **30**(3): 528-537.

[2] JIN H, LI J, LI A Q. Checking calculation of fatigue strength for cast steel joints of offshore tour tower under wave loads [J]. *Journal of Southwest Jiaotong University*, 2010, **45**(5): 692-697 (in Chinese).

[3] JIN H, LI J, MO J H, et al. Fatigue of girth butt weld for cast steel node connection in tower structure under wave loadings [J]. *The Structural Design of Tall and Special Buildings*, 2014, **23**(15): 1119-1140.

[4] GUO Q, HUANG X, HAN Q H, et al. Effective notch stress analysis of butt weld on cast steel joint [J]. *Journal of Civil, Architectural & Environment Engineering*, 2018, **40**(3): 23-30 (in Chinese).

[5] HAN Q, GUO Q, YIN Y, et al. Fatigue performance of butt welds between cast steel joint and steel tubular members [J]. *Fatigue & Fracture of Engineering Materials & Structures*, 2017, **40**(4): 642-651.

[6] HAN Q H, GUO Q, YIN Y, et al. Fatigue behavior of G20Mn5QT cast steel and butt welds with Q345B steel [J]. *International Journal of Steel Structures*, 2016, **16**(1): 139-149.

[7] GUO Q. Experimental research and numerical analysis on fatigue behavior of circular butt welds on cast steel joints [D]. Tianjin, China: Tianjin University, 2015 (in Chinese).

[8] JIN C L. Fatigue analysis of butt welds of cast steel joints based on notch stress approach [D]. Nanjing, China: Southeast University, 2018 (in Chinese).

[9] SUN Y, ZHU L M, WANG L X, et al. Fatigue strength analysis of girth butt weld of cast steel joint with branches based on equivalent structural stress method [J]. *Chinese Journal of Applied Mechanics*, 2019, **36**(1): 183-190 (in Chinese).

[10] GONG W J. Effect of casting defects on mechanical properties of steel structure with cast steel nodes [D]. Nanjing, China: Southeast University, 2016 (in Chinese).

[11] LI K S, WU S. Effect of casting defects on the fatigue properties of steel joints in the construction tubular truss bridge [J]. *Foundry Technology*, 2018, **39**(6): 1188-1191 (in Chinese).

[12] LI K S, WU S. Fatigue analysis on casting defects of cast steel joints [J]. *Foundry Technology*, 2018, **39**(10): 2190-2192 (in Chinese).

[13] ZHU M L, XUAN F Z, DU Y N, et al. Very high cycle fatigue behavior of a low strength welded joint at moderate temperature [J]. *International Journal of Fatigue*, 2012, 40: 74-83.

[14] ZHU M L, XUAN F Z, CHEN J. Influence of microstructure and microdefects on long-term fatigue behavior of a Cr-Mo-V steel [J]. *Materials Science and Engineering A*, 2012, 546: 90-96.

[15] ZHU M L, XUAN F Z. Failure mechanisms and fatigue strength assessment of a low strength Cr-Ni-Mo-V steel welded joint: Coupled frequency and size effects [J]. *Mechanics of Materials*, 2016, **100**: 198-208.

[16] Shenyang Research Institute of Foundry Co., Ltd. Methods for ultrasonic testing and for specifying quality levels of steel castings: GB/T 7233—1987 [S]. Shenyang, China: National Technical Committee on Foundry of Standardization Administration of China, 1987 (in Chinese).

[17] ZHAO S B, WANG Z B. Anti-fatigue design: Methods and data [M]. Beijing, China: Machinery Industry Press, 1997 (in Chinese).

[18] WHEELER J B, HOERSCH H M, MAHY H P, et al. Statistical analysis of fatigue data [M]. Philadelphia, USA: American Society for Testing and Materials, 1981.

[19] JIN H, ZHANG Q L, WANG H J. Check of fatigue strength of members for cast steel node [J]. *Steel Construction*, 2008, **23**(10): 17-21 (in Chinese).

[20] CASTILLO E, HADI A S. Modeling lifetime data with application to fatigue models [J]. *Journal of the American Statistical Association*, 1995, **90**(431): 1041-1054.